9th AUSTRALASIAN
FLUID MECHANICS CONFERENCE
AUCKLAND, 8-12 DECEMBER 1986

Wind Loading on Porous Cladding

J. C. K. CHEUNG and W. H. MELBOURNE

Department of Mechanical Engineering, Monash University, Melbourne, Australia.

ABSTRACT

Wind loads on porous cladding are found to be lower than those on a similar non-porous cladding because air flows through the porous surface into the internal volume, tending to equalise the mean pressures and attenuating the peak pressures across the cladding, both of which can reduce the total wind loading on the cladding. The effects of porosity and internal volume on the mean, standard deviation and peak pressures on a porous surface in a pressure field similar to that for a roof or wall of a building have been measured. Reduction factors based on wind loads on a similar non-porous cladding have been evaluated so that design wind loads on porous cladding can be estimated from external pressure coefficients given in existing wind loading codes.

INTRODUCTION

This paper is a continuation of a research effort, reported at the 2nd Workshop on Wind Engineering and Industrial Aerodynamics in Melbourne (Cheung and Melbourne, 1985), studying the effects of porosity on wind loading on a porous roof in an attempt to enable codification of such wind loads on porous cladding. The previous report established reduction factors to be used in evaluating wind loads from external pressure coefficients for moderately large elemental areas near the leading edge and near the centre of a porous roof. The present investigation extends the previous measurements in determining the wind loads at incremental points across the whole streamwise length on the porous roof. Since the previous results have shown that the external pressure coefficients vary only with the distance from the leading edge, dependent on the external building flow field but independent of the porosity and internal volume, the external pressures were only measured for the fully sealed model in the present series of experiments. Also, the external pressure coefficients when referenced to the pressure directly underneath have previously been shown to be the same as the lift force coefficients obtained from strain gauge balance measurements. Consequently, the coefficients for the pressure difference across the external top and the bottom tapping directly underneath will be presented as equivalent to the lift force coefficient at that location in this paper.

EXPERIMENTAL ARRANGEMENT

A model of a low-rise, flat-roofed building, as shown in Figure 1, was tested in a modelled natural wind in the 2 x 2 m working section of the Boundary Layer Wind Tunnel at Monash University. The blockage ratio is 6%. Although Hunt (1981) has concluded that the effects of blockage on pressure measurements on prismatic buildings are insignificant for blockage ratios less than 10%, this effect will be checked later. No blockage corrections have been made to the data in this paper. The exponent for the mean velocity profile is 0.21 and the turbulence intensity at the model height is 15%. The top of the model was porous with 1156 holes of 1/8" in diameter and 64 holes of 1/16" in diameter uniformly distributed over the area. The roof porosity, being the ratio of the area of the holes to the total area of the roof, was varied by masking off some of the holes with tape. A partition

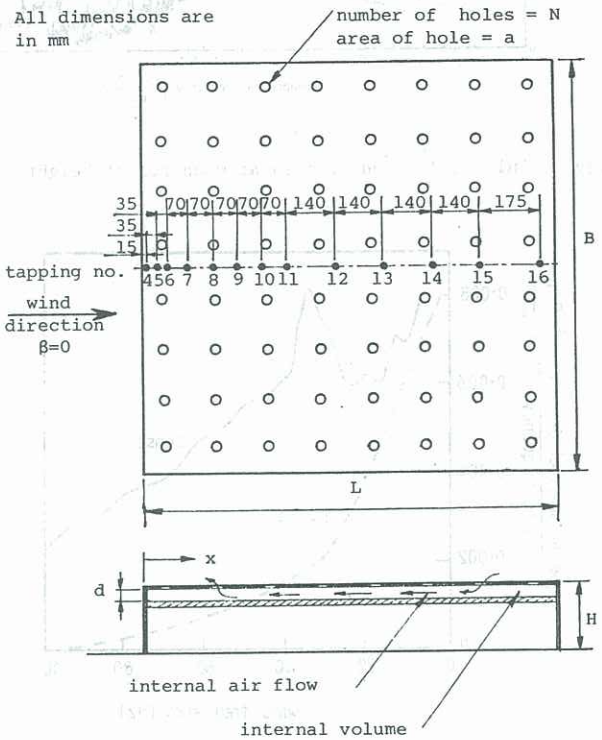

B = breadth of the model = 1210 mm

L = length of the model = 1210 mm

H = height of the model = 200 mm

ε = porosity = $\frac{\text{open area}}{\text{total area}} = \frac{N.a}{B.L}$

μ = internal volume ratio = $\frac{d}{H}$

ρ = density of air

σ = standard deviation

$$C_L = \frac{p_t - p_b}{\frac{1}{2}\rho \bar{u}_H^2}$$

$$C_p = \frac{p_t - p_o}{\frac{1}{2}\rho \bar{u}_H^2}$$

p_t = pressure at top of surface

p_b = pressure at bottom directly underneath

u_H = wind speed at model height H

Superscripts

$\bar{}$ mean

$\hat{}$ maximum peak

$\check{}$ minimum peak

Fig. 1: Nomenclature and dimensions of the model with a porous roof.

was installed inside the model to change the internal volume of the model. The ratio of the depth of the internal volume to the external height of the model is defined as the internal volume ratio relevant to the air flow inside the model. Pressure tappings were placed on top and below the central area of the roof along the entire streamwise length. The top tappings were connected to one channel of the scanivalve while the corresponding bottom tappings were connected to another channel. The channel with bottom tappings was connected to the reference of a Setra pressure transducer monitoring the first channel of the top tappings so that the pressure difference across the roof could be measured for each pair of the top and bottom tappings, scanned along the streamwise length of the model for different porosities and internal volumes. Pressure measurements for the top tappings were repeated with the reference of the Setra pressure transducer connected to the freestream static pressure for the case of zero porosity when the porous holes on the roof of the model were fully sealed with masking tape. The Setra pressure transducers were used together with connecting tube restrictors to ensure that the response to pressure fluctuations on the model were flat up to a frequency of 200 Hz. The output from the pressure transducer was low pass filtered at 280 Hz to cut off any resonance or external noise components. Mean, standard deviation and minimum and maximum peak pressures were measured.

EXPERIMENTAL RESULTS

The definition of the pressure coefficients are given in Figure 1. For the non-porous roof the mean, standard deviation and peak external pressure coefficients referenced to the freestream static pressure are plotted in Figure 2 as a function of the distance from the leading edge. The results agree quite well with the previous measurements (Cheung and Melbourne, 1985) for the regions near the leading edge and the centre of the model and with others (Gerhardt and Kramer, 1983) for building facades. The highest wind loads occur in regions of separated flow near the leading edge of the model and reattachment occurs at a relative distance of about x/L = 0.4.

The external pressure coefficient referenced to the pressure directly underneath was found to be the same as the lift force coefficient from the previous measurements (Cheung and Melbourne, 1985) and hence the lift force coefficients presented in this paper were evaluated from the measurements of the pressure difference across the roof with respect to the dynamic pressure of the upstream wind flow at model height. As the porosity of the roof increases, the porosity allows air to flow through the cladding to the internal volume tending to equalize the mean pressures. Hence the pressure difference across the roof is reduced. The reduction factors, i.e. the ratio of the lift force coefficient to the external pressure

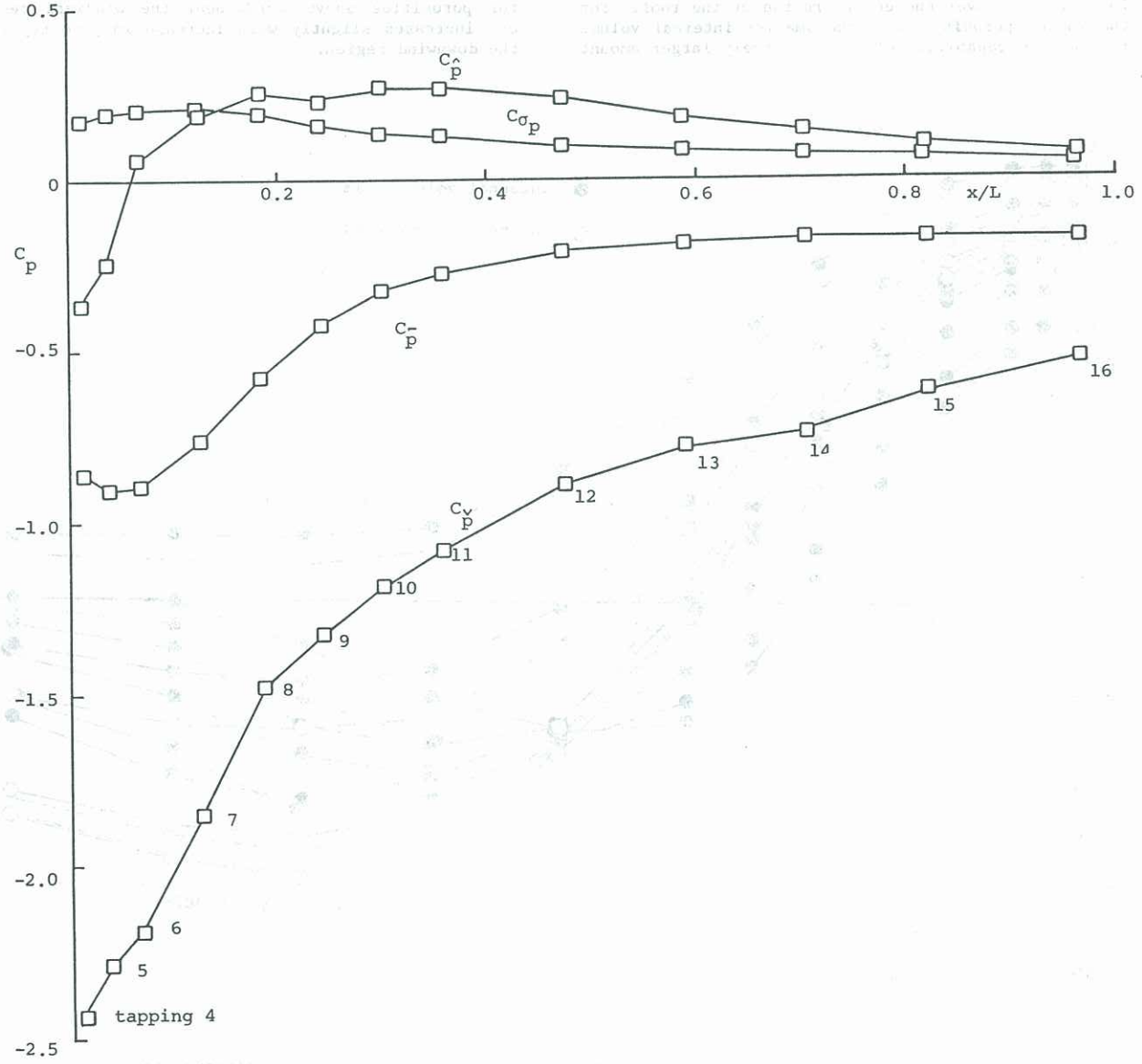

Fig. 2: Mean, standard deviation and peak external pressure coefficients referenced to the freestream static pressure as a function of distance from the leading edge on a non-porous roof.

coefficient referenced to the freestream static pressure is plotted in Figure 3 as a function of distance from the leading edge on the porous roof for different porosities and internal volumes. Even with a small amount of porosity, a negative pressure is induced in the space underneath. Because the air can flow in the internal volume, the highly negative external pressure near the leading edge can induce a relatively high negative internal pressure on the underside of the downstream part of the model roof. As shown in Figure 3, the reduction in wind loads is generally greater further downwind from the leading edge. As the porosity increases further, it becomes more permeable to air flow across the roof. The induced internal pressure on the downwind side becomes so highly negative that the direction of the wind load is reversed. Thus, the net wind load is downward although the external pressure coefficient is negative. For small porosity of less than 0.01%, increase of internal volume reduces the mean wind load. However, as the porosity increases further, the opposite trend occurs for the windward region while for the downwind region the effects remain to be reducing the wind load by increasing the internal volume. This measurement supports an explanation of some inconsistency on the effect of internal volume noted in the earlier work. As for the small porosity, air flow across the permeable roof is so small that even a small internal volume allows the small air flow over the entire area underneath. Therefore, increasing the internal volume only increases the air flow across the porous roof slightly and thus reduces the wind load slightly over the entire region of the roof. For the larger porosity roof, the smaller internal volume reduces the capability of the relatively larger amount of air flowing across the porous roof to flow internally between the windward and downwind regions. The induced high negative internal pressure near the windward region becomes more localized. Hence, more reduction in wind load for the windward region and less reduction for the downwind region can be seen as the internal volume reduces.

This effect of internal volume for different porosities and for different regions of the model can also be seen in Figure 4, the cross plot of Figure 3, of the reduction factor as a function of roof porosity for different tappings and different internal volumes. The mean wind load on the porous roof near the leading edge is shown to be lower by about 20% of that on a non-porous roof when the porosity is 0.08% or above. Except for regions very close to the leading edge, $x/L < 0.02$, this reduction in load can be increased to 40% as porosity increases and internal volume decreases.

Similar reduction factors were evaluated for the minimum peak measurements as shown in Figures 5. The effect of internal volume on the reduction factors for peak measurements is very small. Therefore, the data for each porosity presented in Figure 5 are a best fit curve of the averages for different internal volumes. The peak wind load near the leading edge can be reduced by about 12% on the porous roof as compared to the wind load on a non-porous roof. Further reduction, as much as 30%, can be achieved in the downstream region. The reduction factor remains about the same for porosities above 0.05% near the windward region and increases slightly with increase in porosity near the downwind region.

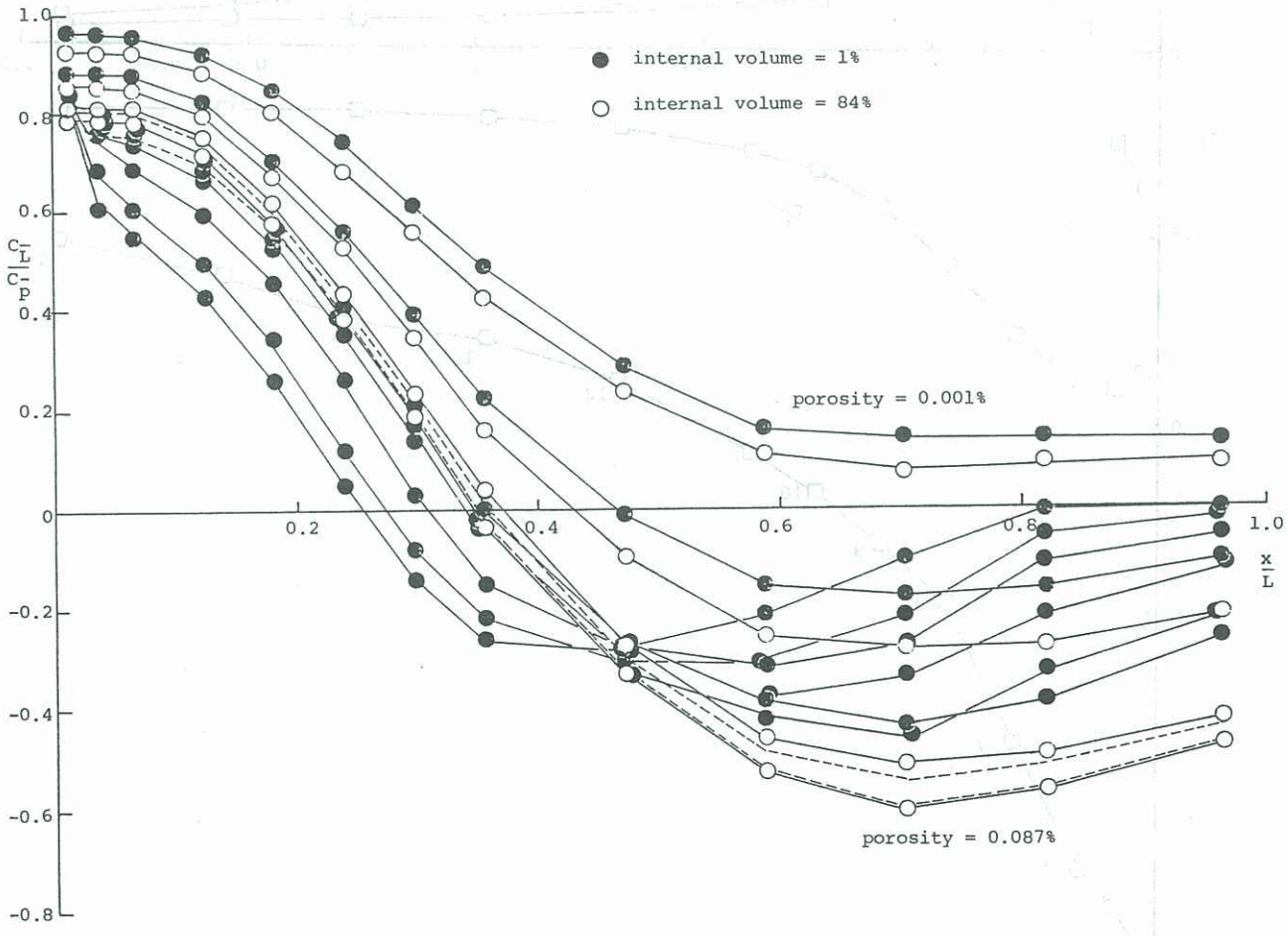

Fig. 3: Ratio of mean lift coefficient to mean pressure coefficient as a function of distance from the leading edge on the porous roof for different porosities and internal volumes.

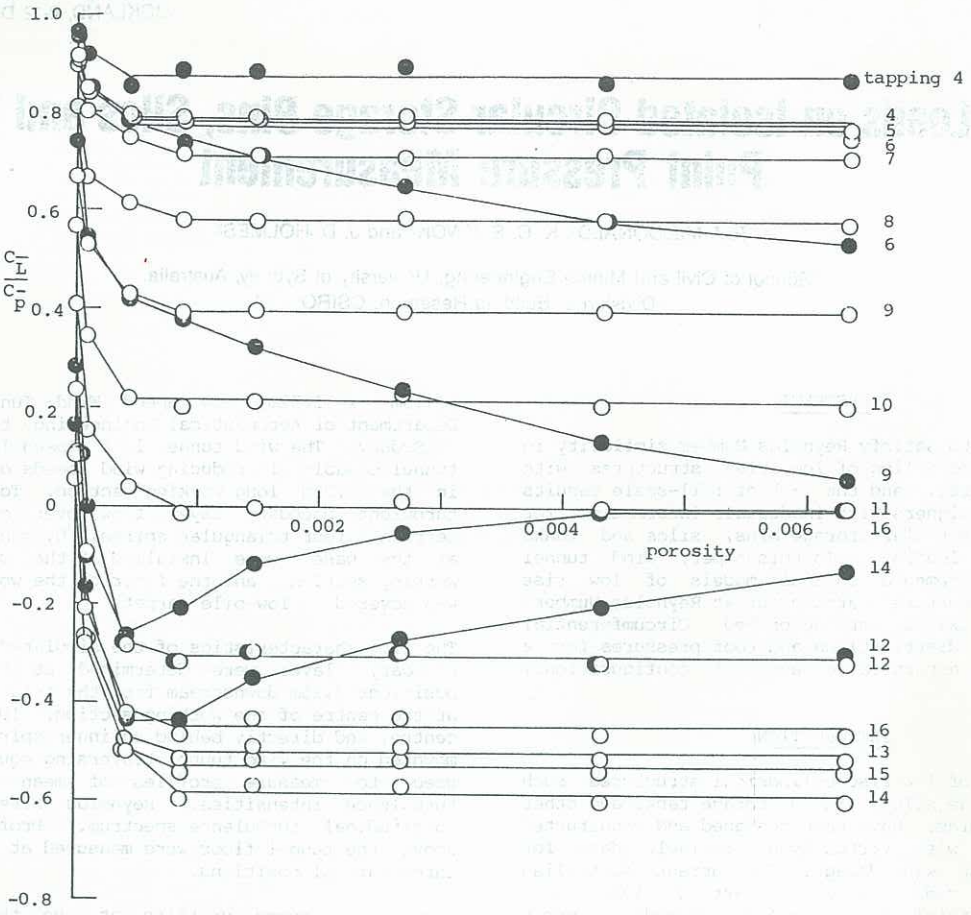

Fig. 4: Ratio of mean lift coefficient to mean pressure coefficient as a function of roof porosity for different tappings and different internal volumes.

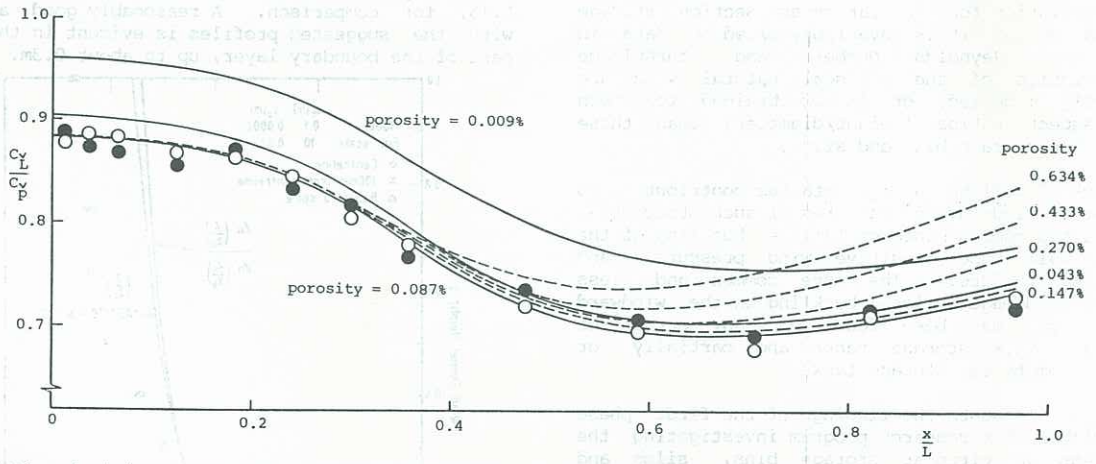

Fig: 5 Ratio of minimum peak lift coefficient to minimum peak pressure coefficient as a function of distance from the leading edge on the porous roof for different porosities and internal volumes.

CONCLUSIONS

Wind loads on porous cladding are found to be lower than those on a similar non-porous cladding because air flow through the porous surface induces a negative pressure in the internal volume. The effects of porosity and internal volume on the wind load reduction have been quantified for the centre region along the entire streamwise length of the roof. Reduction factors to facilitate the evaluation of design wind loads on porous cladding from external pressure coefficient data have been developed for a typical low-pitch roof cladding for normal wind direction. This conclusion leads to further research which includes the effects of various roof pitch angles and different wind directions.

REFERENCES

Cheung, J C K and Melbourne, W H (1985): Wind loading on porous cladding. Proc. of the 2nd Workshop on Wind Engineering and Industrial Aerodynamics, CSIRO, Melbourne.

Hunt, A (1981): Scale effects on wind tunnel measurements of wind effects on prismatic buildings. Ph.D. Thesis, Cranfield Institute of Technology.

Gerhardt, H J and Kramer, C (1983): Wind loads on wind-permeable building facades. Jnl. Wind Eng. and Ind. Aerodynamics, 11, 1-20.